

Final Report

Title: Gallium nitride UV single photon source

AFOSR/AOARD Reference Number: FA2386-09-1-4062

AFOSR/AOARD Program Manager: Dr. John Seo

Period of Performance: 2008.08.01 – 2010.07.31

Submission Date: 2010.11.08

PI: Seong-Ju, Park (Gwangju Institute of Science and Technology (GIST))

Report Documentation Page

Form Approved
OMB No. 0704-0188

Public reporting burden for the collection of information is estimated to average 1 hour per response, including the time for reviewing instructions, searching existing data sources, gathering and maintaining the data needed, and completing and reviewing the collection of information. Send comments regarding this burden estimate or any other aspect of this collection of information, including suggestions for reducing this burden, to Washington Headquarters Services, Directorate for Information Operations and Reports, 1215 Jefferson Davis Highway, Suite 1204, Arlington VA 22202-4302. Respondents should be aware that notwithstanding any other provision of law, no person shall be subject to a penalty for failing to comply with a collection of information if it does not display a currently valid OMB control number.

1. REPORT DATE 12 NOV 2010		2. REPORT TYPE FInal		3. DATES COVERED 01-09-2009 to 30-09-2010	
4. TITLE AND SUBTITLE Gallium nitride UV single photon source				5a. CONTRACT NUMBER FA23860914062	
				5b. GRANT NUMBER	
				5c. PROGRAM ELEMENT NUMBER	
6. AUTHOR(S) Seong-Ju Park				5d. PROJECT NUMBER	
				5e. TASK NUMBER	
				5f. WORK UNIT NUMBER	
7. PERFORMING ORGANIZATION NAME(S) AND ADDRESS(ES) Gwangju Institute of Science and Technology,1 Oryongdong, Bukgu,Gwangju 500-712,Korea,KR,500712				8. PERFORMING ORGANIZATION REPORT NUMBER N/A	
9. SPONSORING/MONITORING AGENCY NAME(S) AND ADDRESS(ES) AOARD, UNIT 45002, APO, AP, 96337-5002				10. SPONSOR/MONITOR'S ACRONYM(S) AOARD	
				11. SPONSOR/MONITOR'S REPORT NUMBER(S) AOARD-094062	
12. DISTRIBUTION/AVAILABILITY STATEMENT Approved for public release; distribution unlimited					
13. SUPPLEMENTARY NOTES					
14. ABSTRACT This report documents the development of electrically driven single photon source that operate near room temperature by using epitaxially grown GaN nanostructures. In order to realize the electrically driven single photon source operating near room temperature, we grew high-quality GaN quantum dots embedded in AlN thin films, and fabricate single photon emitting tunnel diodes that have GaN quantum dots in a microcavity structure with nano-sized aperture. Single electron and hole injection, which is the precondition for single photon emission, was driven by using Coulomb blockade effect in GaN quantum dots surrounded by AlN tunnel barriers.					
15. SUBJECT TERMS Optoelectronic Materials, nanoelectronics					
16. SECURITY CLASSIFICATION OF:			17. LIMITATION OF ABSTRACT Same as Report (SAR)	18. NUMBER OF PAGES 47	19a. NAME OF RESPONSIBLE PERSON
a. REPORT unclassified	b. ABSTRACT unclassified	c. THIS PAGE unclassified			

1. Objectives

In this project, the overall objectives are developments of electrically driven single photon source that operate near room temperature by using epitaxially grown GaN nanostructures. In order to realize the electrically driven single photon source operating near room temperature, we will grow high-quality GaN quantum dots embedded in AlN thin films, and fabricate single photon emitting tunnel diodes that have GaN quantum dots in a microcavity structure with nano-sized aperture. Single electron and hole injection, which is the precondition for single photon emission, will be driven by using Coulomb blockade effect in GaN quantum dots surrounded by AlN tunnel barriers. Figure 1 shows a schematic of the proposed single photon emitting diode.

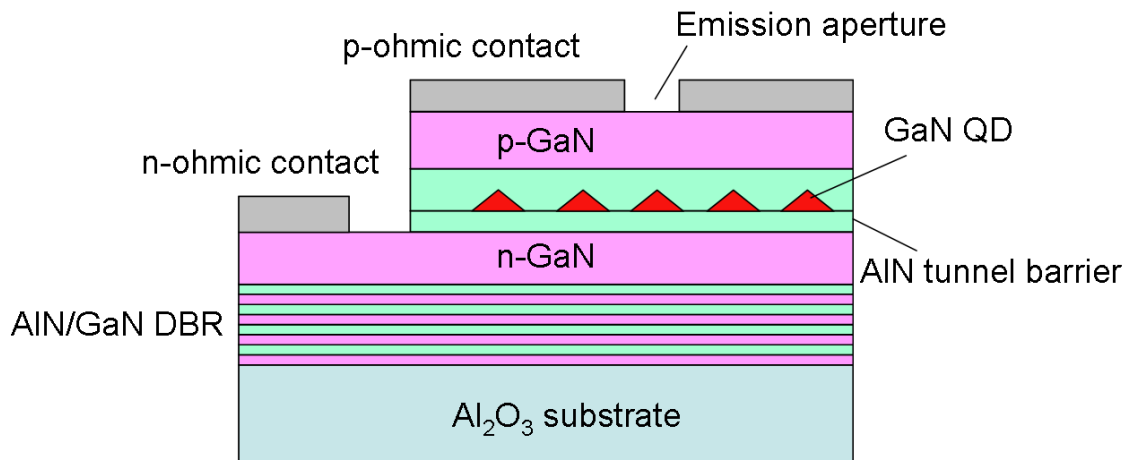


Figure 1. Schematic diagram of the proposed single photon emitting diode

This proposal aims to develop the electrically driven single photon sources for applications in quantum computing and quantum cryptography. The development of single photon devices is an important issue and has much potential in the field of modern photonics and optical technology in conjunction with nanotechnology.

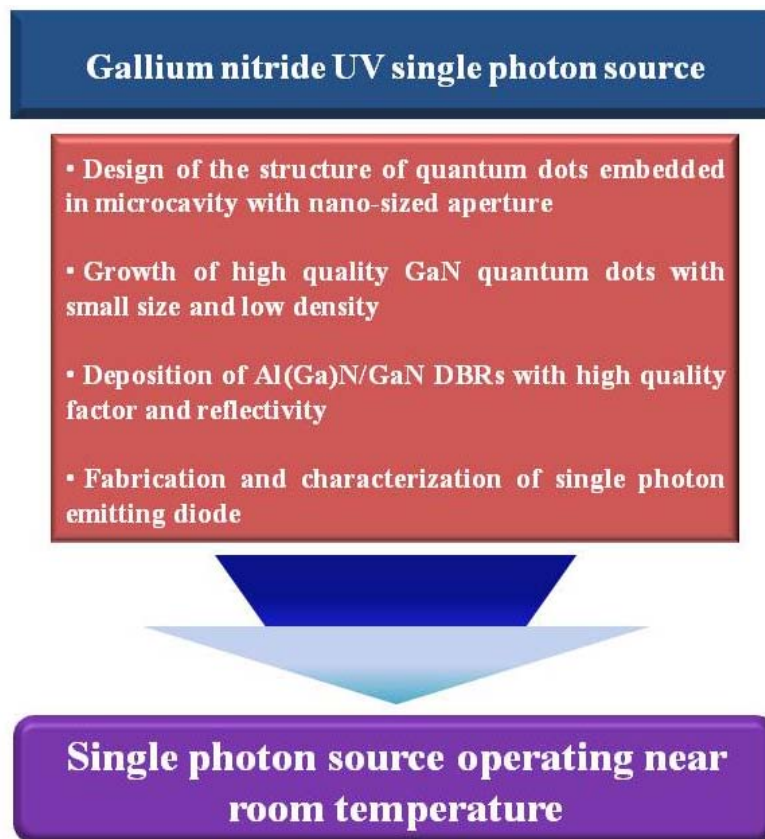


Figure 2. Research structure for the development of single photon source

Electrically driven single photon sources operating at room temperature have for many years been desirable devices in the fields of quantum optics, optical quantum computing, and quantum cryptography. Our suggested devices, in this proposal, can be used in developing practical quantum computers and secure optical communication channels with commercial significance.

2. Status of effort

We have designed the structure for single photon emitting devices that have GaN nanostructures embedded into the microcavity structure. The design of the device structure was accomplished using Rsoft FULLWAVE simulation. In order to realize the electrically driven single photon sources, we have grown InGaN quantum dots with small size and low density using metalorganic chemical vapor deposition (MOCVD). Additionally, Al(Ga)N/GaN heterostructures with high quality are grown because it is important for the high performance of single photon emitting diodes. The optical cavity structure will be applied to develop an efficient single photon source. The growth condition of Al(Ga)N/GaN distributed Bragg Reflectors (DBRs) have been optimized for the microcavity structure. Furthermore, we tried to characterize the emission from quantum dots embedded in a microcavity.

3. Abstract

We have grown InGaN quantum dots on GaN layer by the Stranski-Krastanow (S-K) growth mode using MOCVD under the various growth conditions for quantum dots with a small size of a few nanometers and low density of $\sim 10^9/\text{cm}^2$. Since the growth of InGaN quantum dots is very sensitive to the growth condition, the formation of InGaN quantum dots can be controlled by growth parameter such as the growth temperature, time and the flow rate of MO sources. Especially, InGaN quantum dots with small size and low density are required to realize electrically driven single photon sources. InGaN quantum dots are characterized by using AFM and photoluminescence (PL) measurement to analyze the structural and optical properties. Additionally, it is required to embed InGaN quantum dots into the microcavity with a small volume and high quality factor for a high internal quantum efficiency and photon collection efficiency of single photon emitters. We have optimized Al(Ga)N/GaN distributed Bragg Reflectors (DBRs) for a cavity mode and 38% of reflectivity can be obtained using 5 pairs of $\text{Al}_{0.2}\text{Ga}_{0.8}\text{N}/\text{GaN}$ DBRs instead of 30 pairs of DBRs.

4. Personnel Supported

Name	ID No.	Affiliation	Position (Status)	Start Date	Project Participation Ratio (%)
		Department	Field of Study/ Final Degree	End Date	
Park, Seong- Ju	521101- 1023317	GIST	Professor	20080801	30
		MSE	Semiconductor/ Ph.D.	20100731	
Cho, Chu- Young	810224- 1068931	GIST	Ph.D. course	20080801	40
		MSE	Semiconductor/ M.S.	20100731	
Lee, Sang- Jun	820814- 1581013	GIST	Ph.D. course	20080801	40
		MSE	Semiconductor/ M.S.	20100731	
Hong, Sang- Hyun	810831- 1274215	GIST	Ph.D. course	20090801	40
		MSE	Semiconductor/ M.S.	20100731	

Park, Seung- Chul	801024- 1522719	GIST	M.S. course	20080801	30
		MSE	Semiconductor / B.S.	20100731	
Jeong, Seung- Hui	831209- 2646112	GIST	Assistant	20080801	20
		MSE	Electronics/B.E.	20100731	

5. Publications

"Enhancement of light extraction from GaN-based green light-emitting diodes using selective area photonic crystal", Kim *et al.*, Applied Physics Letters, **96**, 251103 (2010)

"Growth of height-controlled InGaN quantum dots on GaN" – Park *et al.*, Journal of crystal growth, **312**, 2065 (2010)

"Improvement of efficiency droop in InGaN/GaN multiple quantum well light-emitting diodes with trapezoidal wells", Han *et al.*, Journal of Physics D: Applied Physics, **43**, 354004 (2010)

"Surface plasmon-enhanced light-emitting diodes using silver nanoparticles embedded in p-GaN", Cho *et al.*, Nanotechnology, **21**, 205201 (2010)

"Enhanced light extraction in light-emitting diodes with photonic crystal structure selectively grown on p-GaN" – Cho *et al.*, Applied Physics Letters, **96**, 181110 (2010)

"Effect of Mg doping in the barrier of InGaN/GaN multiple quantum well on optical power of light-emitting diodes", Han *et al.*, Applied Physics Letters, **96**, 051113 (2010)

"Improvement of GaN-based light-emitting diodes using p-type AlGaIn/GaN superlattices with a graded Al composition" – submitted in Journal of Physics D: Applied Physics

"Effect of electron-blocking layer on efficiency droop in InGaN/GaN multiquantum well light-emitting diodes" – Han *et al.*, Applied Physics Letters, **94**, 231123 (2009)

6. Interactions

(a) 6th US-KOREA workshop on nanoelectronics

Date: 19-20 May 2009

Place: Hanyang University, Seoul, Korea

Title: Gallium Nitride UV Single Photon Source

Abstract: The overall objectives of our research are developments of electrically driven single photon source that operates near room temperature by using epitaxially grown GaN nanostructures. In order to realize the electrically driven single photon source operating near room temperature, we first grow the high-quality InGaN quantum dots (QDs) embedded in AlN thin films. For the InGaN QDs embedded in AlN films, a high quality of AlN layer was obtained at high temperature by using metal-organic chemical vapor deposition (MOCVD). After the growth of AlN epilayer, InGaN QDs on an AlN epilayer were demonstrated by the Stranski-Krastanow (S-K) growth mode. The structural and optical properties of InGaN QDs were analyzed by using atomic force microscopy (AFM) and photoluminescence (PL) measurement, respectively. In addition, we demonstrated a cavity mode by using AlN/GaN pairs as distributed Bragg reflectors (DBRs). AlN/GaN DBRs was optimized by using a simulation program (Rsoft FULLWAVE), and the thickness of each epilayer can be calculated by following equation, $d = \lambda/4n$, where d and λ are the thicknesses of

epilayer and wavelength, respectively. The characteristics of the emission from InGaN QDs embedded in a microcavity will be discussed.

(b) Electrically driven single photon sources operating at room temperature have for many years been desirable devices in the fields of quantum optics, optical quantum computing, and quantum cryptography. Our suggested devices, in this proposal, can be used in developing practical quantum computers and secure optical communication channels with commercial significance.

7. Inventions

None

8. Honors/Awards

Academic awards of Korean Vacuum Society (2009)

9. Archival Documentation

1) Design of the devices

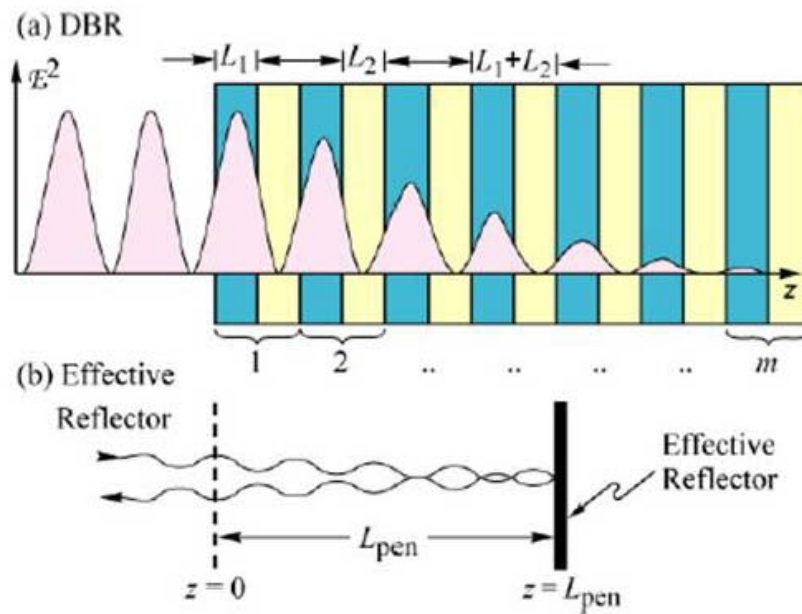
In order to develop an efficient single photon source, it is required to embed quantum dots into the microcavity with a small volume and high quality factor. As a result, high quality quantum dots embedded in a microcavity structure can be applied to collect single photon emission.

We demonstrate a cavity mode by using $\text{Al}_{0.2}\text{Ga}_{0.8}\text{N}/\text{GaN}$ pairs as distributed Bragg Reflectors (DBRs). The refractive index of GaN and $\text{Al}_{0.2}\text{Ga}_{0.8}\text{N}$ is 2.53 and 2.4 [Appl. Phys. Lett. **70**, 3209 (1997), MRS Internet J. Nitride Semicond. **4S1**, G5.2 (1999)]. The thickness of each epilayer can be calculated by following equation, $d = \lambda / 4n$, where d and λ are the thicknesses of epilayer and wavelength, respectively. Therefore, the thickness of GaN and AlGa_N is given by (at the wavelength of 400 nm)

$$L_{\text{GaN}} = \frac{\lambda}{4n_{\text{GaN}}} = 39.5\text{nm}$$

$$L_{\text{AlGaN}} = \frac{\lambda}{4n_{\text{AlGaN}}} = 41.7\text{nm}$$

Figures 3 (a) and (b) show the schematic diagram of DBRs structure and penetration depth. The DBRs structure consists of two materials with thickness L_1 and L_2 . As shown in Fig. 3 (b), the ideal (metallic) reflector should be displaced from the DBRs surface by the penetration depth.



Figures 3. (a) DBRs consisting of two materials with thickness L_1 and L_2 and (b) Effective reflector by the penetration depth

For a large number of pairs, the penetration depth is given by

$$L_{pen} = \frac{L_{GaN} + L_{AlGaN}}{4} \frac{n_{GaN} + n_{AlGaN}}{n_{GaN} - n_{AlGaN}} = 770nm$$

The effective length of a cavity consisting of two DBRs is given by the sum of the thickness of the center region plus two penetration depths in DBRs.

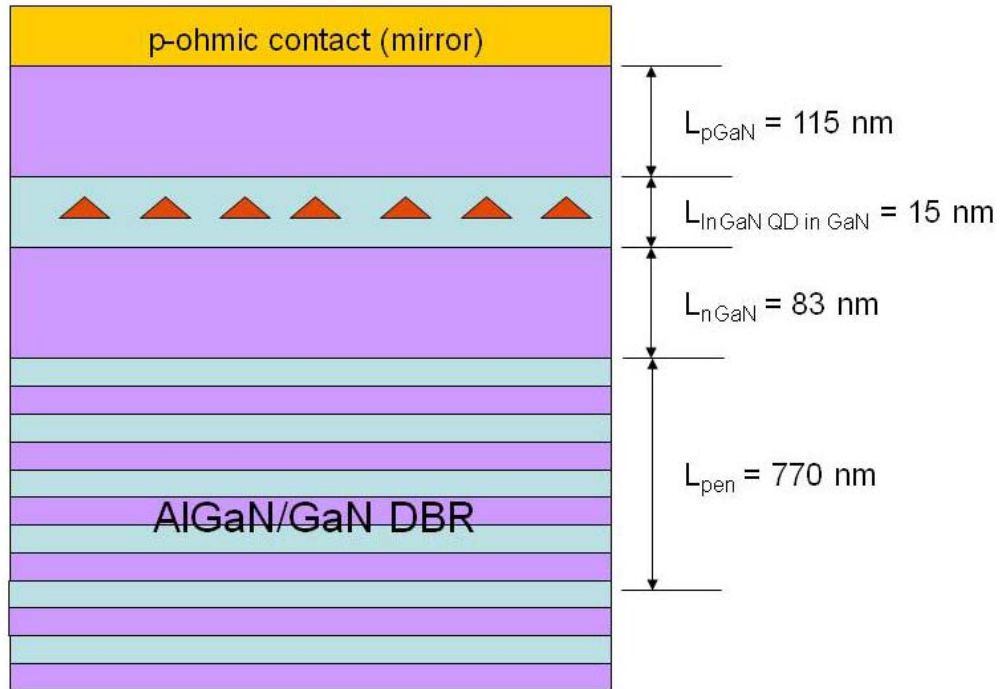


Figure 4. Schematic diagram of the single photon device structure

Based on the calculation, the full-structure for single photon source is designed as shown in Fig. 4. AlGaIn/GaN DBRs consist of 30 pairs and the reflectivity is expected to be over 90 %. The InGaIn quantum dots are embedded in GaN layer with a thickness of 15 nm. The *n*-type and *p*-type GaN can be deposited as an electron and hole injection layer, respectively.

When the cavity mode number, *m* is 12, the cavity length is given by

$$L_{\text{cavity}} = m\lambda/2n = L_{\text{pen}} + L_{\text{nGaIn}} + L_{\text{pGaIn}} + L_{\text{QD/GaN}} = 983 \text{ nm}$$

The position of quantum dots layer should be applied at the maximum electric field in the cavity length. Figure 5 shows the electric field as a growth direction in the cavity length. The quantum dots layer is positioned at 122 nm from the top of cavity.

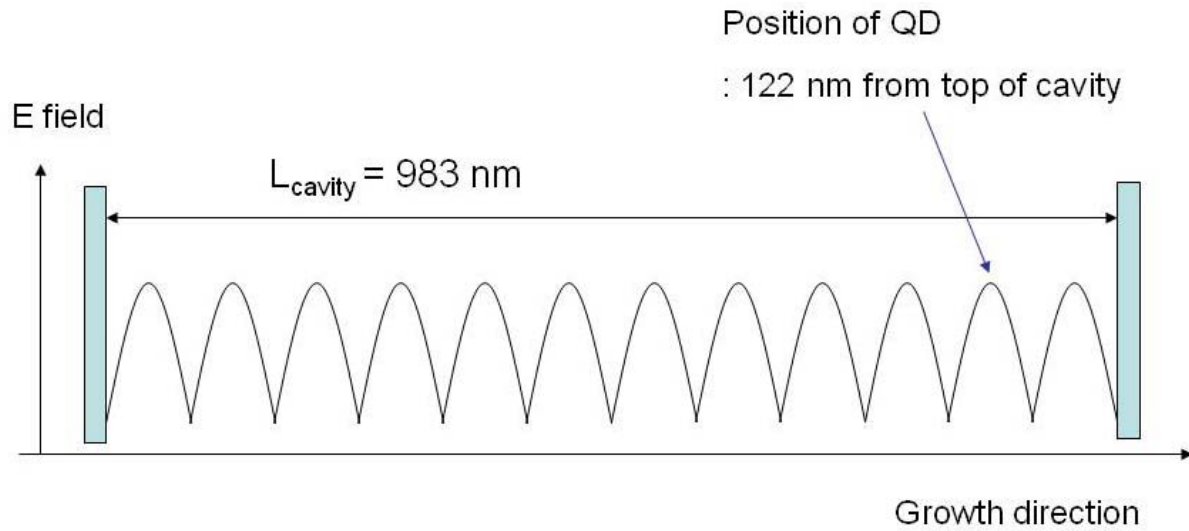
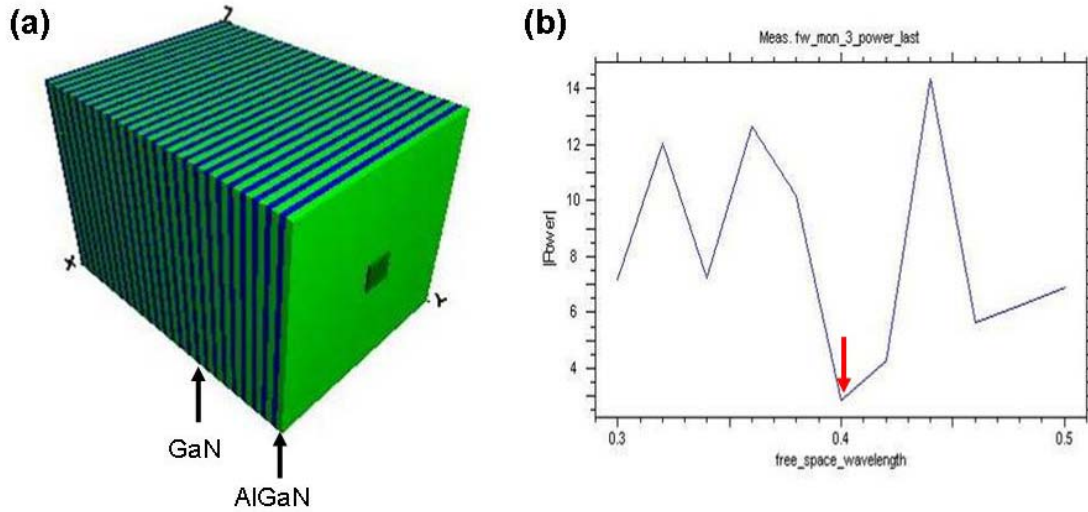


Figure 5. Electric field as a growth direction in the cavity length

2) Simulation of the devices

The design of single photon device structure is accomplished using Rsoft FULLWAVE simulation. The objectives of this simulation are to confirm the reflectance of DBRs and alignment of the maximum electric field with quantum dots.

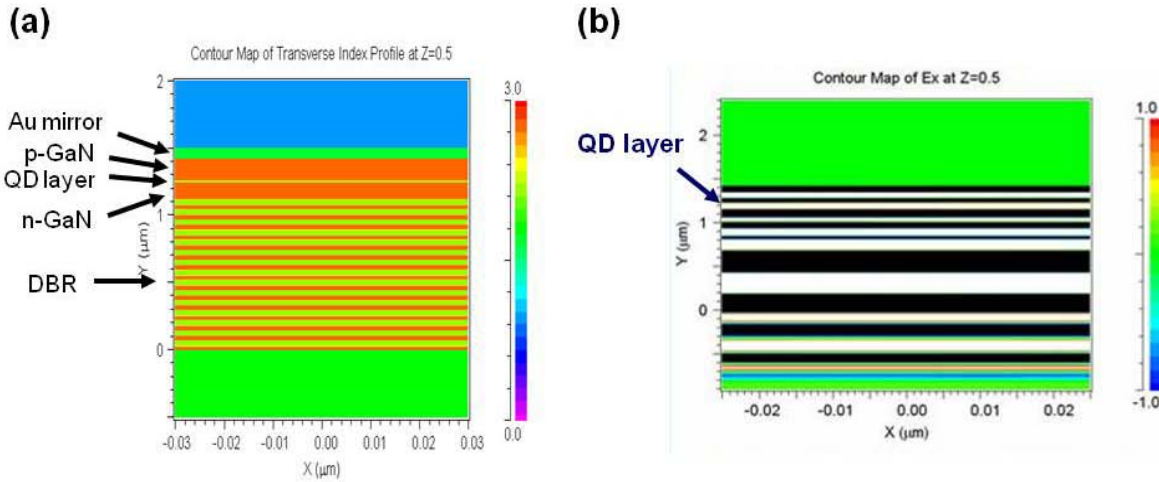


Figures 6. (a) Simulation structure for 30 pairs of AlGaIn/GaN DBRs and (b) Simulated transmittance

Figures 6 (a) and (b) show the simulation structure for 30 pairs of AlGaIn/GaN DBRs and simulated transmittance. The composition of Al is 20 % in AlGaIn layer and the calculated thickness of each layer (AlGaIn/GaN) is 41.7 nm and 39.5 nm, respectively for the target wavelength of 400 nm. The simulated transmittance is lowest at the wavelength of 400 nm as shown in Fig. 6 (b). This indicates that the light cannot be transmitted after propagating 30 pairs of AlGaIn/GaN DBRs at wavelength of 400 nm. The reflectivity of 30 pairs of AlGaIn/GaN DBRs is about 94%.

Figures 7 (a) and (b) show the refractive index and electric field profile of device structure. The refractive index of each layer is considered at 400 nm and Au layer is used

as upper DBRs for the microcavity structure. The position of quantum dots layer is 122 nm from top of cavity that has a maximum electric field as shown in Fig. 7 (b).



Figures 7. (a) Refractive index and (b) Electric field profile of the device structure

Figure 8 is the light intensity from the device structure as a function of wavelength. Based on Fig. 8, the resonant wavelength is 400 nm inside the cavity. Therefore, the simulation result is comparable to the calculated result.

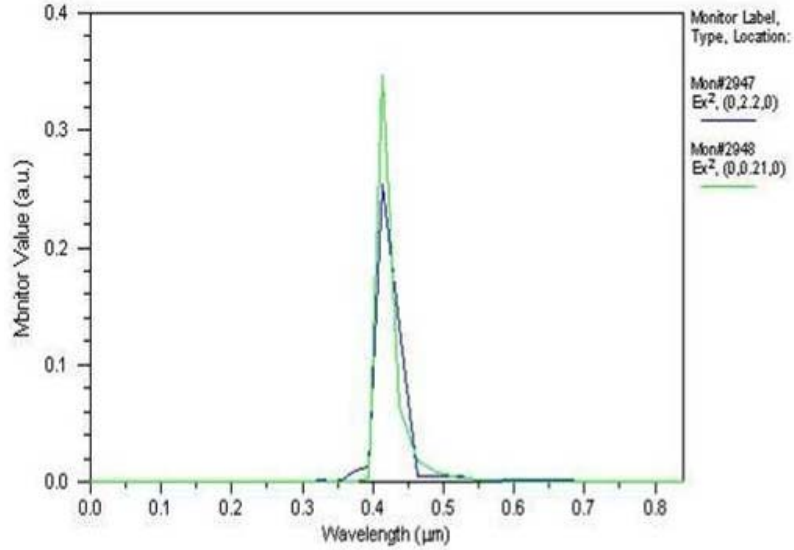


Figure 8. Light intensity from the device structure as a function of wavelength

3) Growth and characterization

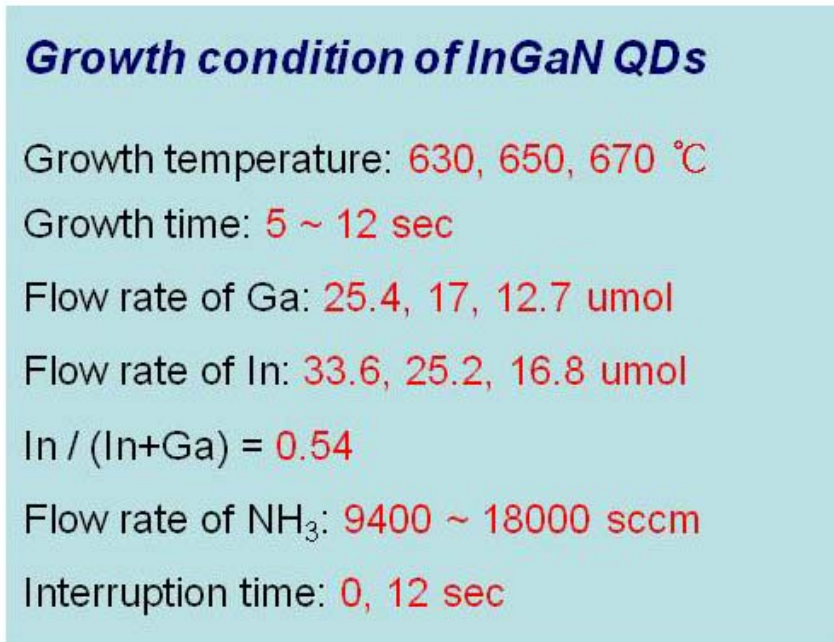
In order to control single photon emission, charging energy should be small. The charging energy, E_c is given by

$$E_c = \frac{e^2}{C} \quad C \sim 4\pi\epsilon_r d$$

Since d is the size of quantum dots, the charging energy can be increased by reducing the size of quantum dots. Additionally, it is easy to collect the emission from one dot if

the density of quantum dots is low. Therefore, the quantum dots with high quality, small size, and low density are necessary for the higher single photon emission efficiency and large charging energy.

The InGaN quantum dots are grown on GaN layer by Stranski-Krastanow (S-K) growth mode using MOCVD. Table 1 shows the growth condition for InGaN quantum dots on GaN layer. The flow rate of NH₃ is kept without MO source during an interruption time



Growth condition of InGaN QDs

Growth temperature: 630, 650, 670 °C

Growth time: 5 ~ 12 sec

Flow rate of Ga: 25.4, 17, 12.7 umol

Flow rate of In: 33.6, 25.2, 16.8 umol

In / (In+Ga) = 0.54

Flow rate of NH₃: 9400 ~ 18000 sccm

Interruption time: 0, 12 sec

Table 1. Growth condition for InGaN quantum dots on GaN

Figure 9 shows the AFM images of InGaN quantum dots grown on GaN layer as a function of the growth rate. The quantum dots is formed and agglomerated on the GaN surface as the growth rate is decreased.

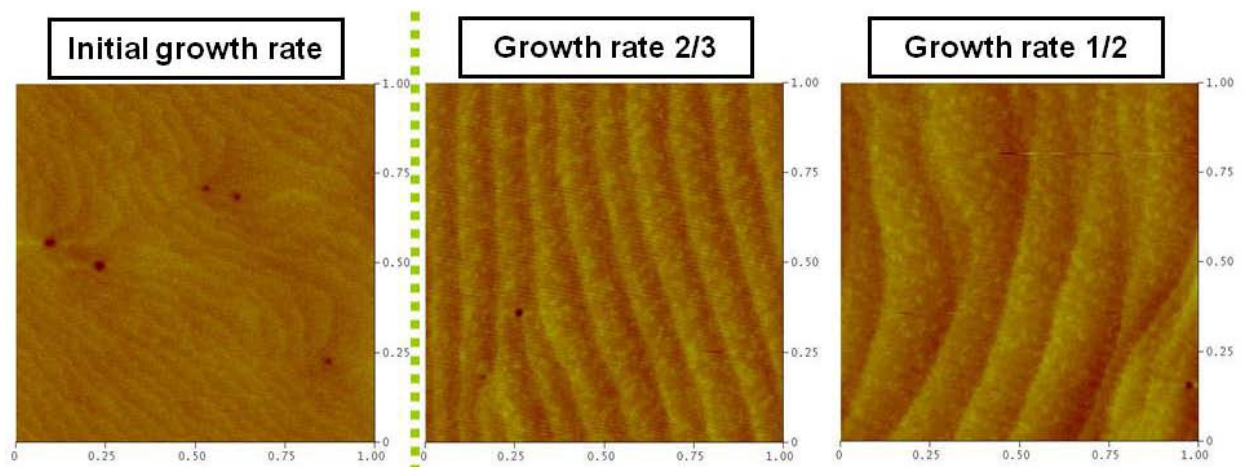
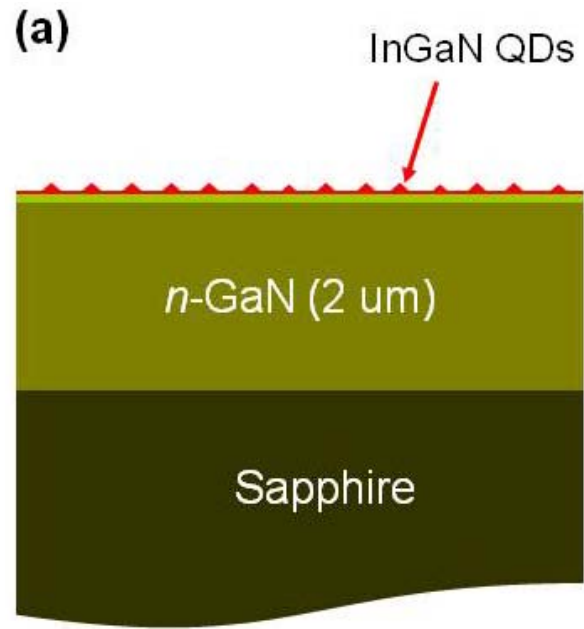
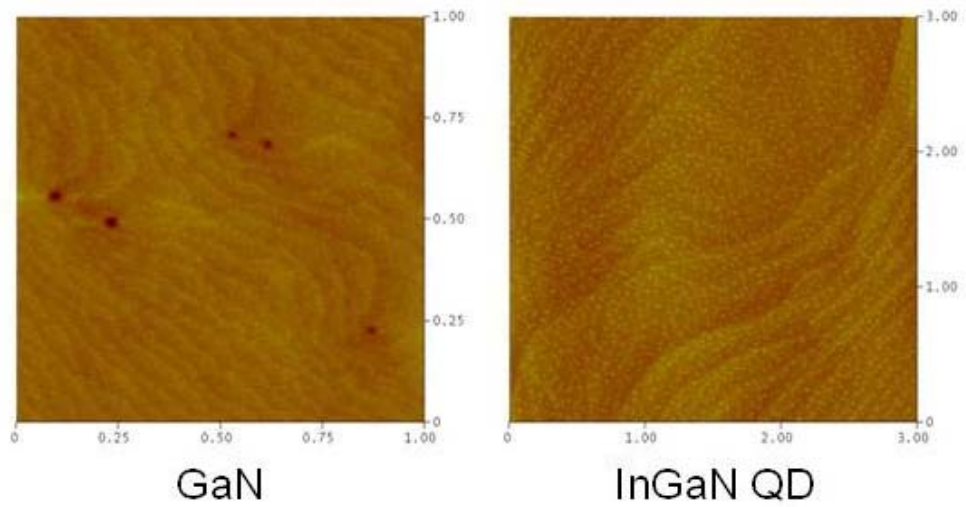


Figure 9. AFM images of InGaN quantum dots grown on GaN layer as a function of the growth rate

Figures 10 (a) and (b) show the schematic diagram for the quantum dots structure and AFM images of GaN layer and InGaN quantum dots.



(b)



Figures 10. (a) Schematic diagram for the quantum dots structure and (b) AFM images of GaN layer and InGaN quantum dots

The GaN layer shows an atomically flat surface for the formation of quantum dots as shown in Fig. 10 (b). The growth temperature and time is 670 °C and 10 sec, respectively. The interruption time is applied before the growth of quantum dots. The density of InGaN quantum dots is about $1 \times 10^{10} / \text{cm}^2$.

The InGaN quantum dots should have a small size and low density to control the single photon emission. Figure 11 shows the AFM images of InGaN quantum dots on GaN layer as a function of growth time. The formation of quantum dots is incomplete at the growth time of 7 sec and the quantum dots starts to form from 9 sec. Total density of InGaN quantum dots is increased up to $\sim 10^{10} / \text{cm}^2$ with increasing the growth time. The size and height of InGaN quantum dots are 20~30 nm and 1~2 nm, respectively indicating that aspect ratio is small.

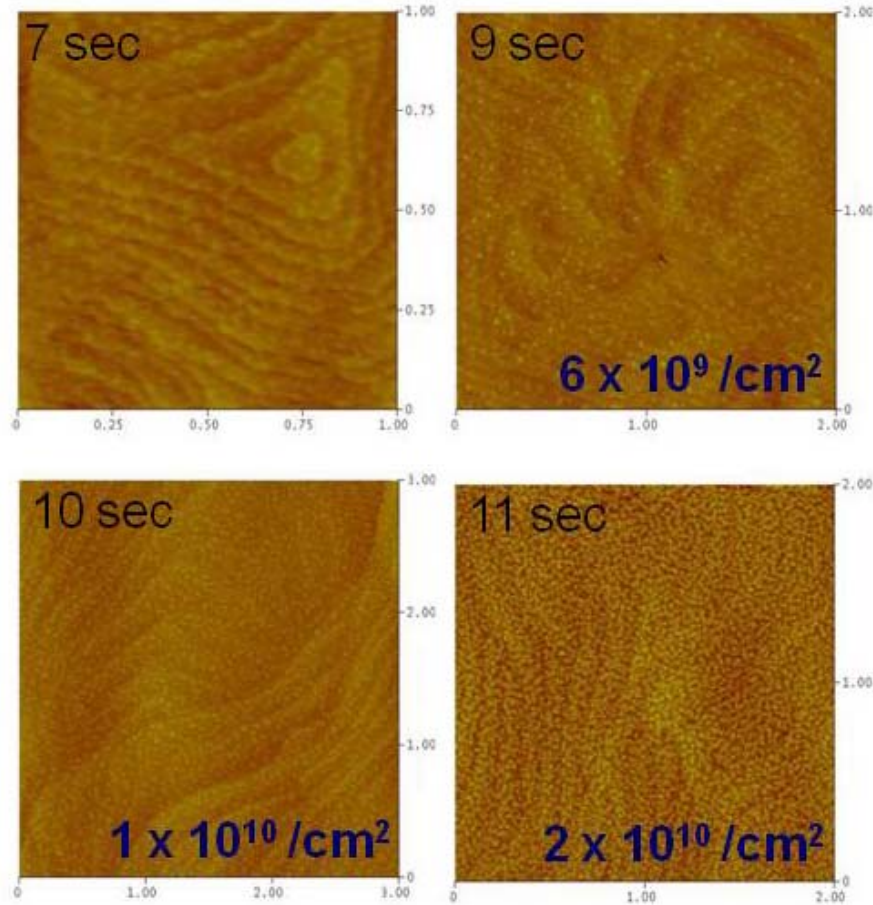
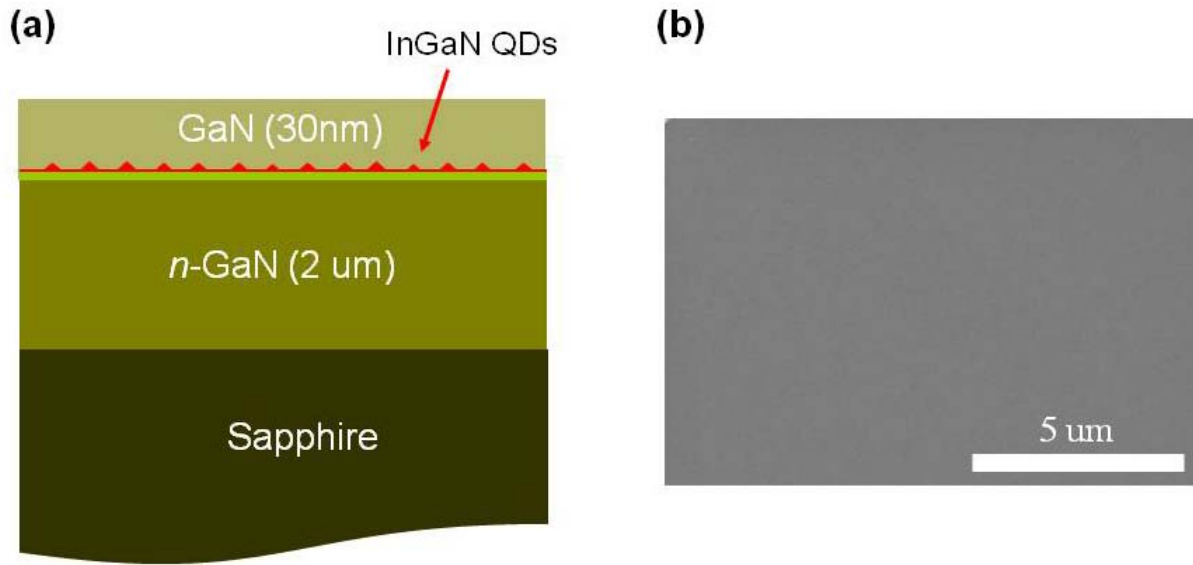


Figure 11. AFM images of InGaN quantum dots grown on GaN layer as a function of growth time

After the growth of InGaN quantum dots, the GaN film was deposited as a capping layer for the characterization of quantum dots. Figures 12 (a) and (b) show the schematic diagram of InGaN quantum dots embedded in GaN capping layer and SEM image of GaN capping layer.



Figures 12 (a) Schematic diagram of InGaN quantum dots embedded in GaN capping layer and (b) SEM image of GaN capping layer

The growth temperature of GaN layer is 750 °C due to the high miscibility of In. The thickness of capping layer is expected to be 30 nm and V/III ratio is 4485. As shown in Fig. 12 (b), GaN capping layer has a smooth surface indicating that InGaN quantum dots are well embedded in GaN.

Figure 13 shows the photoluminescence (PL) measurement of InGaN quantum dots embedded in GaN layer. There is no peak when the formation of quantum dots is

incomplete but the peak near 400 nm is clearly observed after the complete growth of quantum dots

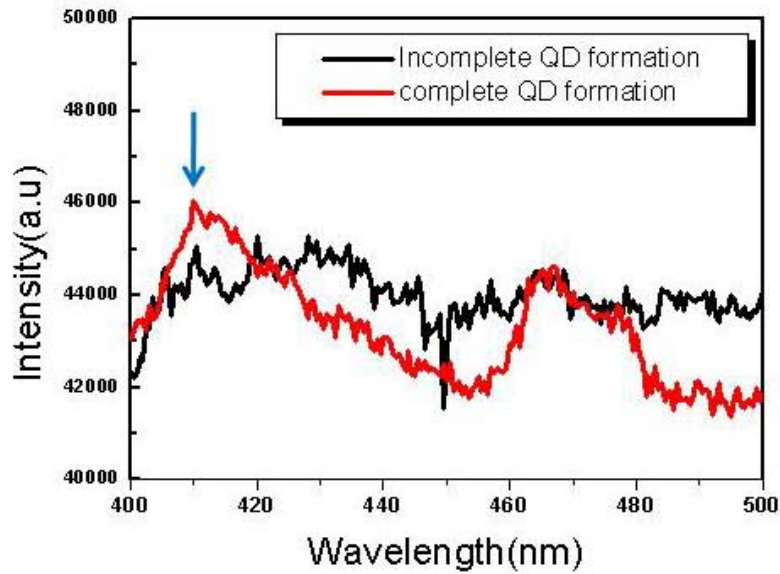


Figure 13. PL measurement of InGaN quantum dots embedded in GaN layer

Figure 14 shows the PL measurement of InGaN quantum dots embedded in GaN layer as a function of flow rate of NH_3 . The PL intensity is slightly increased with increasing a flow rate of NH_3 because 3D growth is dominant under N-rich condition.

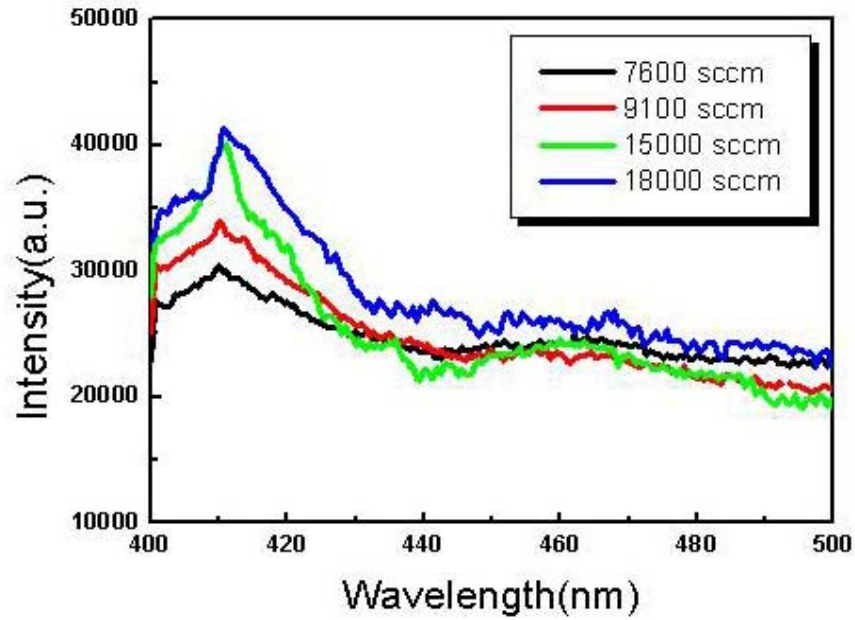
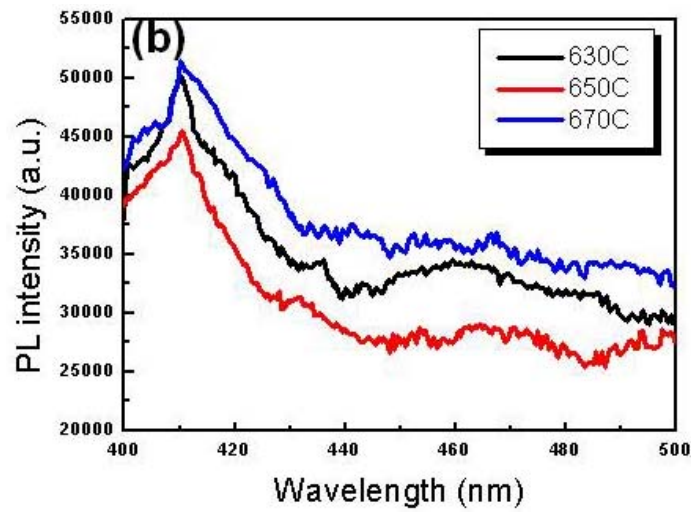
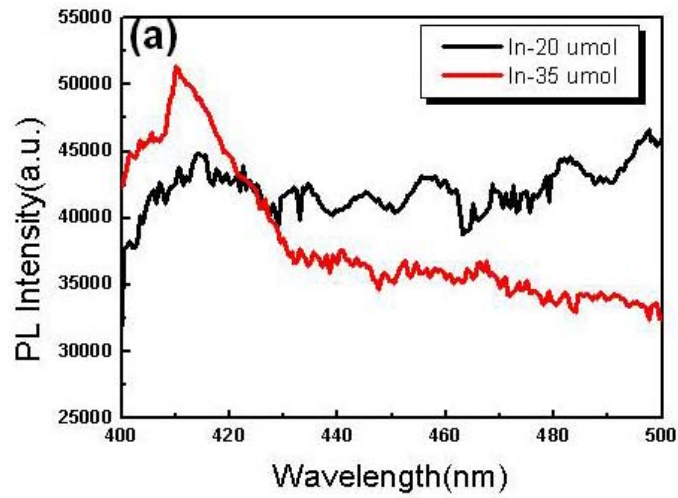
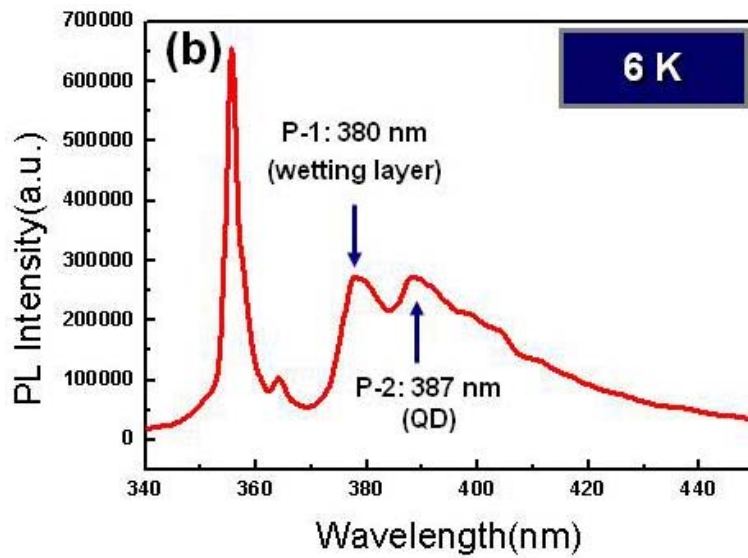
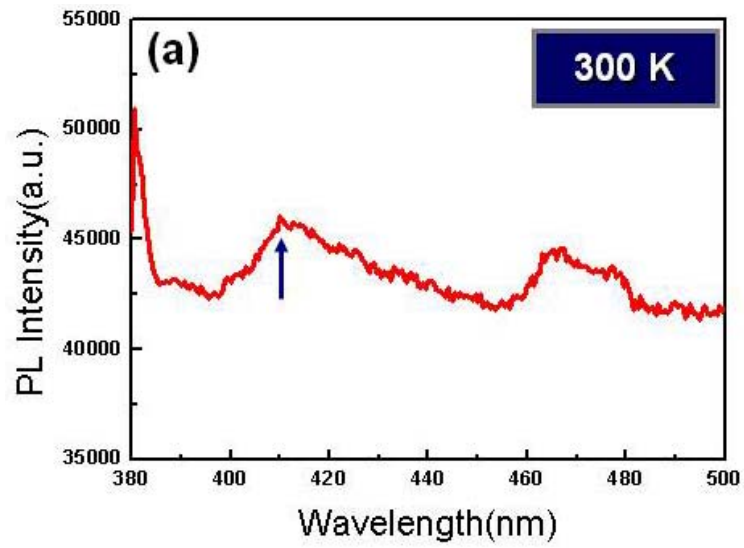


Figure 14. PL measurement of InGaN quantum dots embedded in GaN layer as a function of flow rate of NH_3

Figures 15 (a) and (b) show the PL measurement of InGaN quantum dots embedded in GaN layer as a function of flow rate of TMIIn and growth temperature, respectively. When the flow rate of TMIIn is 20 μmol , there is no peak due to the incomplete formation of quantum dots. The PL peak of quantum dots is observed with increasing a flow rate of TMIIn up to 35 μmol . As shown in Fig. 15 (b), the PL intensities of quantum dots are similar at the growth temperature from 630 $^\circ\text{C}$ to 670 $^\circ\text{C}$.



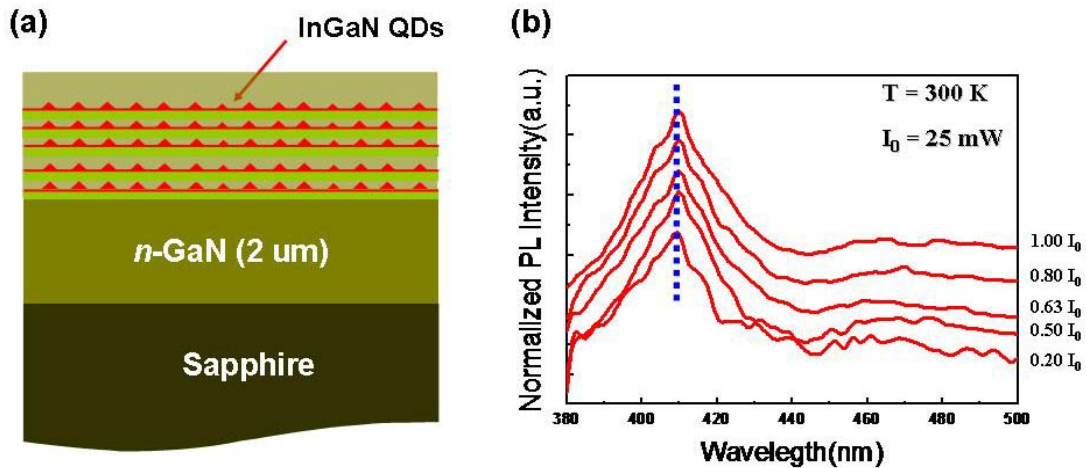
Figures 15. PL measurement of InGaN quantum dots embedded in GaN layer as a function of (a) flow rate of TMIn and (b) growth temperature



Figures 16. PL measurement of InGaN quantum dots with single layer (a) at 300K (room temperature) and (b) at 6K

Figures 16 (a) and (b) show the PL measurement of InGaN quantum dots with single layer at 300K (room temperature) and 6K. The PL peak at 300K shows the wavelength near 400 nm. There are two peaks observed at 6 K. The P-1 (380 nm) and P-2 (387 nm) are from the wetting layer and quantum dots, respectively. Additionally the P-1 cannot be measured at 300 K since carriers in the wetting layer vanish at nonradiative recombination centers such as defect.

Figures 17 (a) and (b) show the schematic diagram of InGaN quantum dots with 5 pairs and PL measurement of this sample as a function of excitation power.



Figures 17. (a) Schematic diagram of InGaN quantum dots with 5 pairs and (b) PL measurement as a function of excitation power

The growth temperature of InGaN quantum dots and GaN capping layer is 670 °C and 750 °C, respectively. There is no blue shift of peak wavelength with excitation power as shown in Fig. 17 (b). This result is attributed to the small quantum-confined Stark effect (QCSE) and negligible piezoelectric field in InGaN quantum dots.

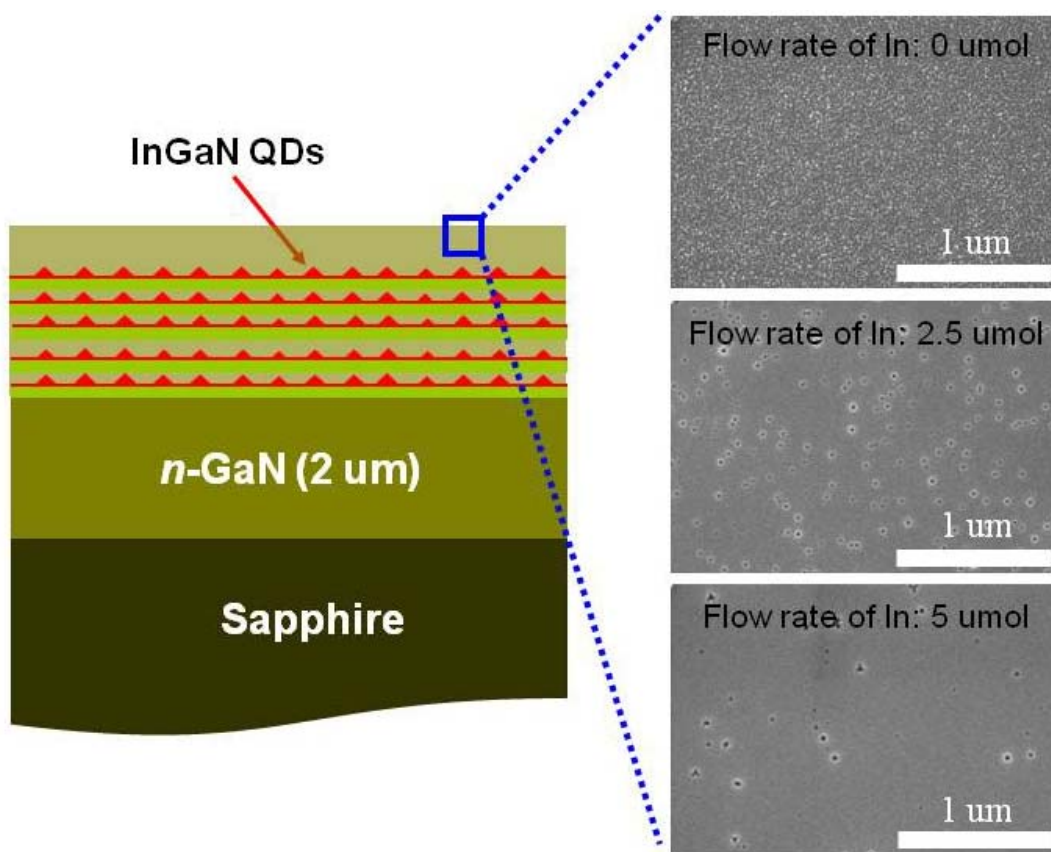
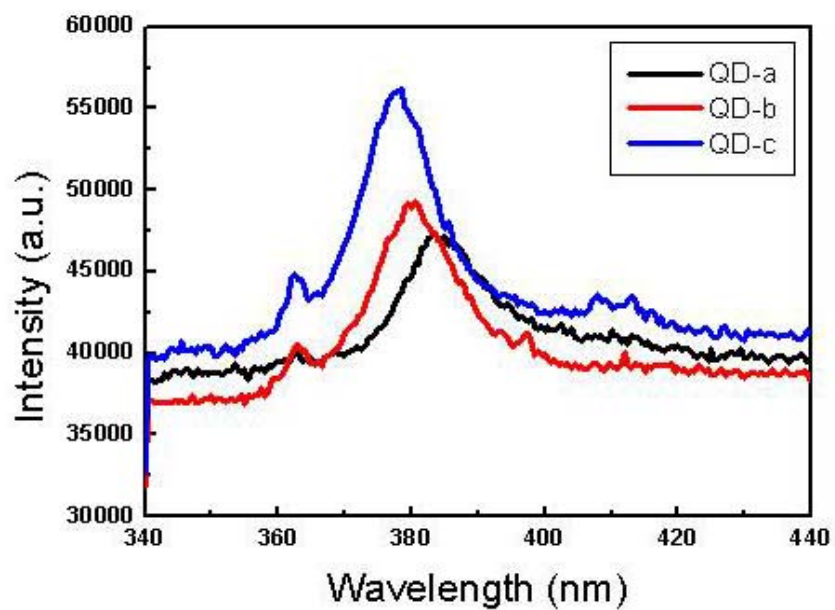


Figure 18. SEM images of GaN capping layer as a function of the flow rate of TMIn in GaN capping layer

The GaN capping layer is formed with rough surface at lower growth temperature (750 °C) under ambient N₂ gas [Phys. Status Solidi C. 6, S561 (2009)]. As a result, the PL emission intensity from quantum dots can be decreased due to the GaN capping layer with a low quality. Indium is used to enhance the structural property of GaN as a surfactant [Appl. Phys. Lett., 73, 2642 (1998)].

Figure 18 shows the SEM images of GaN capping layer as a function of the flow rate of TMIn in GaN capping layer. When there is no flow of TMIn during the growth of GaN capping layer, the surface is degraded with many pit density. However, the pit density is decreased as the flow rate of TMIn increases.

Figure 19 is the PL measurement of InGaN quantum dots embedded in GaN layer with and without a flow rate of TMIn. The PL emission intensity is increases with a higher flow rate of TMIn. Additionally, the full width at half maximum (FWHM) value is decreased. These results indicate that In act as a surfactant for improving the crystal quality of GaN capping layer.

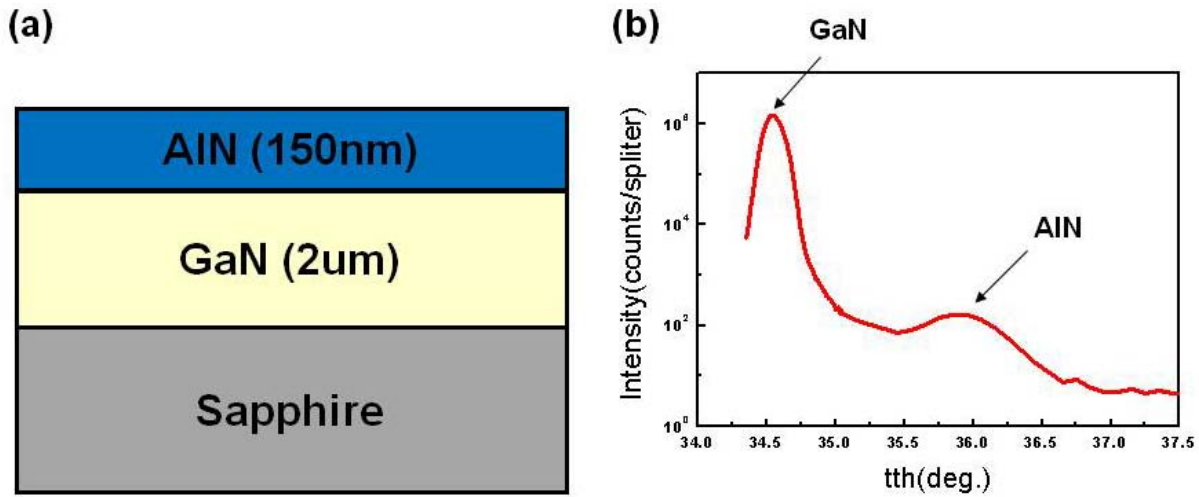


	Flow rate of In (umol)	In/(In+Ga)	FWHM (nm)
QD-a	0	0	12.6
QD-b	2.5	0.13	9.6
QD-c	5	0.23	9.5

Figure 19. PL measurement of InGaN quantum dots embedded in GaN layer with and without a flow rate of TMIIn

In order to develop an efficient single photon source, an optical cavity structure should be fabricated by using Al(Ga)N/GaN DBRs. Because Al(Ga)N/GaN heterostructure has a high refractive index contrast, the high reflectivity can be attained by increasing a number of pairs as shown in the simulation data. The refractive index of AlGaN (n_{AlGaN}) and GaN (n_{GaN}) is 2.4 and 2.53 at the target wavelength of 400 nm. Therefore, the thickness of each layer (L_{AlGaN} and L_{GaN}) is calculated to be 41.7 and 39.5 nm, respectively.

Figures 20 (a) and (b) show the schematic diagram of AlN grown on GaN and XRD measurement of AlN/GaN heterostructure.



Figures 20. (a) Schematic diagram of AlN grown on GaN and (b) XRD measurement of AlN/GaN heterostructure

Trimethyl aluminum (TMAI) and NH_3 are used as sources for Al and N, respectively. The growth temperature and pressure for AlN layer is 1050 and 200 torr. The GaN and AlN peaks are observed in the XRD data.

Figure 21 shows the SEM images of AlN/GaN heterostructure as a function of growth pressure.

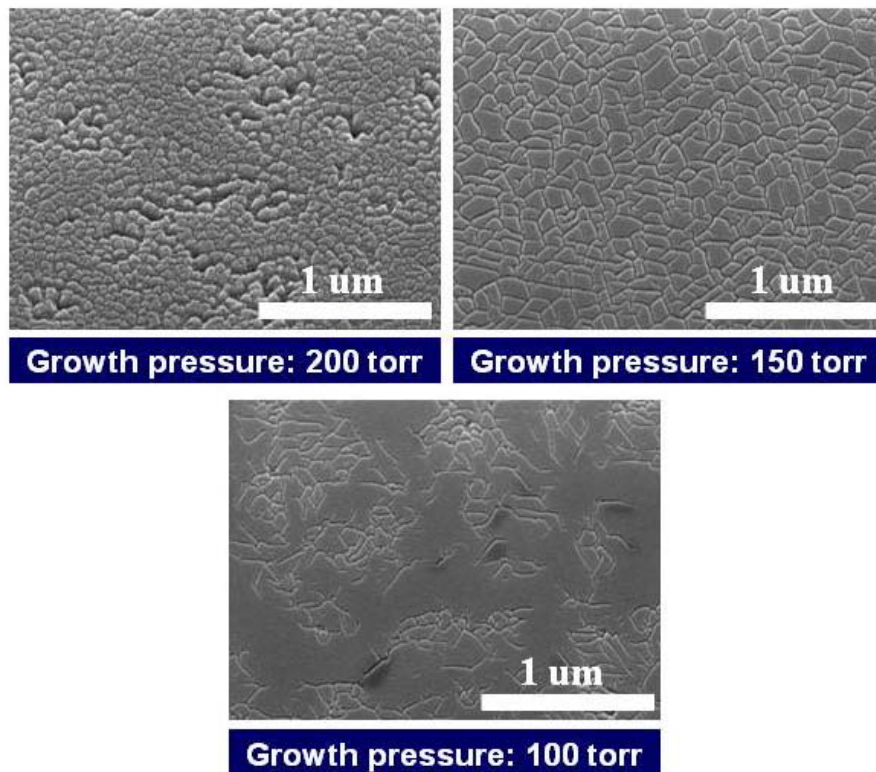


Figure 21. SEM images of AlN/GaN heterostructure as a function of growth pressure

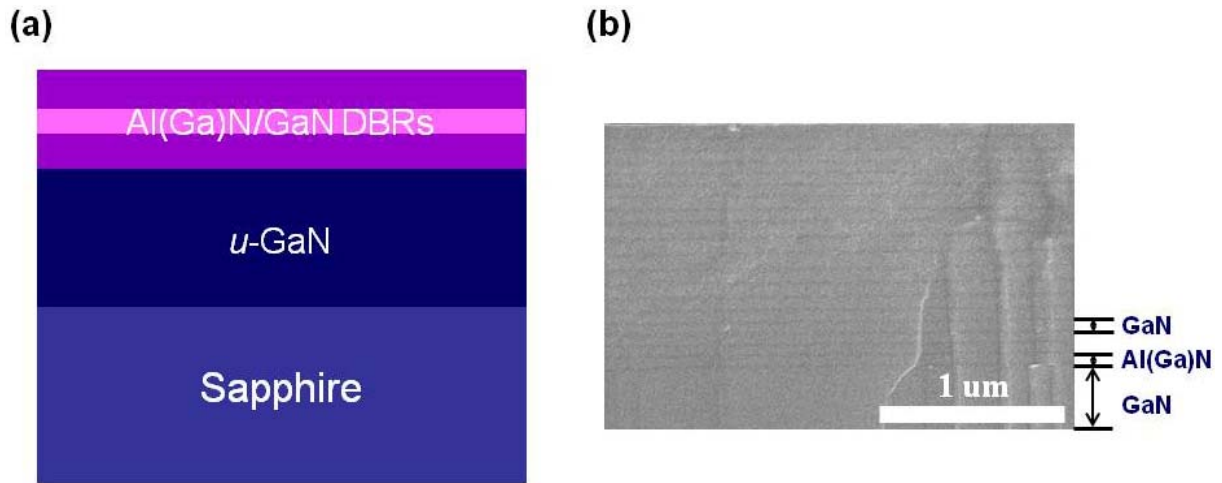
It is important to grow high quality AlN/GaN heterostructure for DBRs. However, crack problem occurs because there is a strain due to the lattice mismatch between GaN and AlN. This can lead to the decrease in reflectivity of DBRs. The surface morphology is improved with decreasing a growth pressure.

Table 2 is the growth condition for Al(Ga)N/GaN DBRs structure. The experiments are performed using 5 pairs of DBRs instead of 30 pairs. The interruption time is applied during the film growth to increase the low surface mobility of Al atom. Furthermore, Indium is used as a surfactant to enhance the surface morphology of AlN films as reported in the previous session.

Figures 22 (a) and (b) show the schematic diagram and SEM image of Al(Ga)N/GaN DBRs. The growth temperature and pressure are 1050 °C and 200 torr for DBRs structure. A sharp interface is observed between AlGa_N and GaN layer. Also, the each pair of AlGa_N/GaN has a thickness comparable to the calculated value.

	Growth pressure	Flow rate of TMGa	Flow rate of TMAI	Flow rate of NH ₃	Interruption time	In surfactant
DBR05	100 Torr	X (AlN)	88 umol	7600 sccm	6 sec	10 umol
DBR06				4400 sccm		
DBR07	150 Torr					
DBR08	200 Torr					
DBR09	150 Torr	106 umol	66 umol	7600 sccm	12 sec	15 umol
DBR10		67 umol				
DBR11		106 umol				
DBR12		67 umol				
DBR13		200 Torr				
DBR14		150 Torr				
DBR15	106 uol	88 umol				
DBR16	53 umol					

Table 2. Growth condition for Al(Ga)N/GaN DBRs structure



Figures 22 (a) Schematic diagram and (b) SEM image of Al(Ga)N/GaN DBRs

Figure 23 shows the SEM images of AlGaIn/GaN DBRs which were grown with increasing a flow rate of TMIIn. Keller *et al.* reported the Indium-surfactant-assisted growth of AlN-GaN multilayer structures by MOCVD [Appl. Phys. Lett., **79**, 3449 (2001)]. However, no effect of In surfactant is observed on the AlN-GaN structures as shown in figure, indicating that the specific composition of In is needed for the growth of AlN using In as the surfactant.

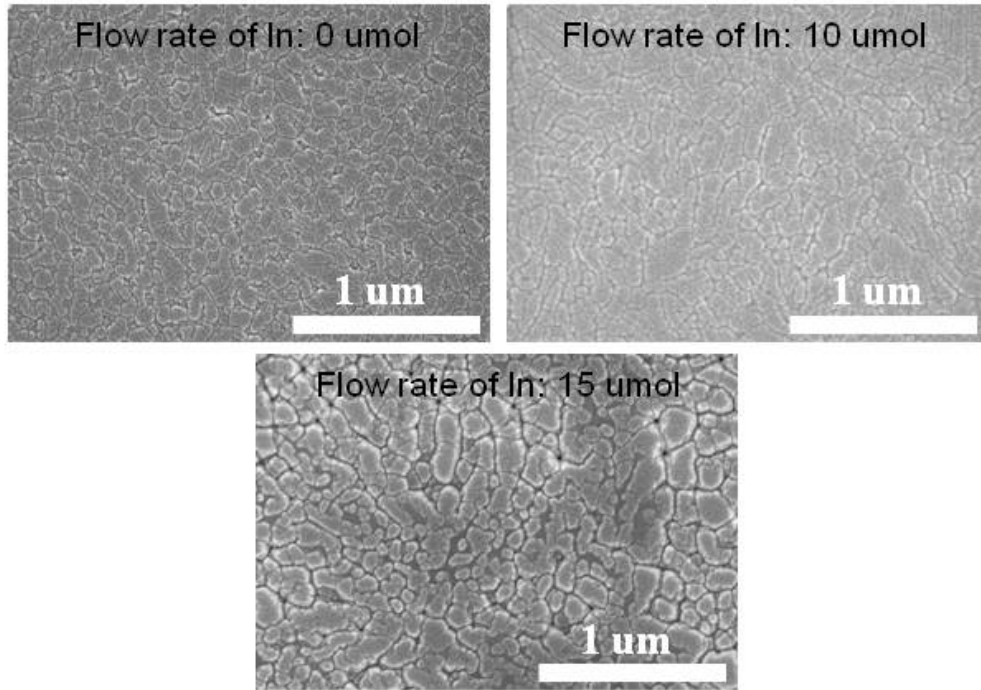


Figure 23. SEM images of AlGaIn/GaN DBRs with a flow rate of TMIIn

Figure 24 shows the SEM images of 5 pairs of AlN/GaN and AlGaIn/GaN DBRs structures, respectively. In case of AlN/GaN DBRs, there is a crack on the surface with growth pressure. This is due to the large lattice mismatch between GaN and AlN.

However, AlGaIn/GaN DBRs structures have a smooth surface without crack because the lattice mismatch is reduced. The Al composition of AlGaIn layer in DBRs is about 20%.

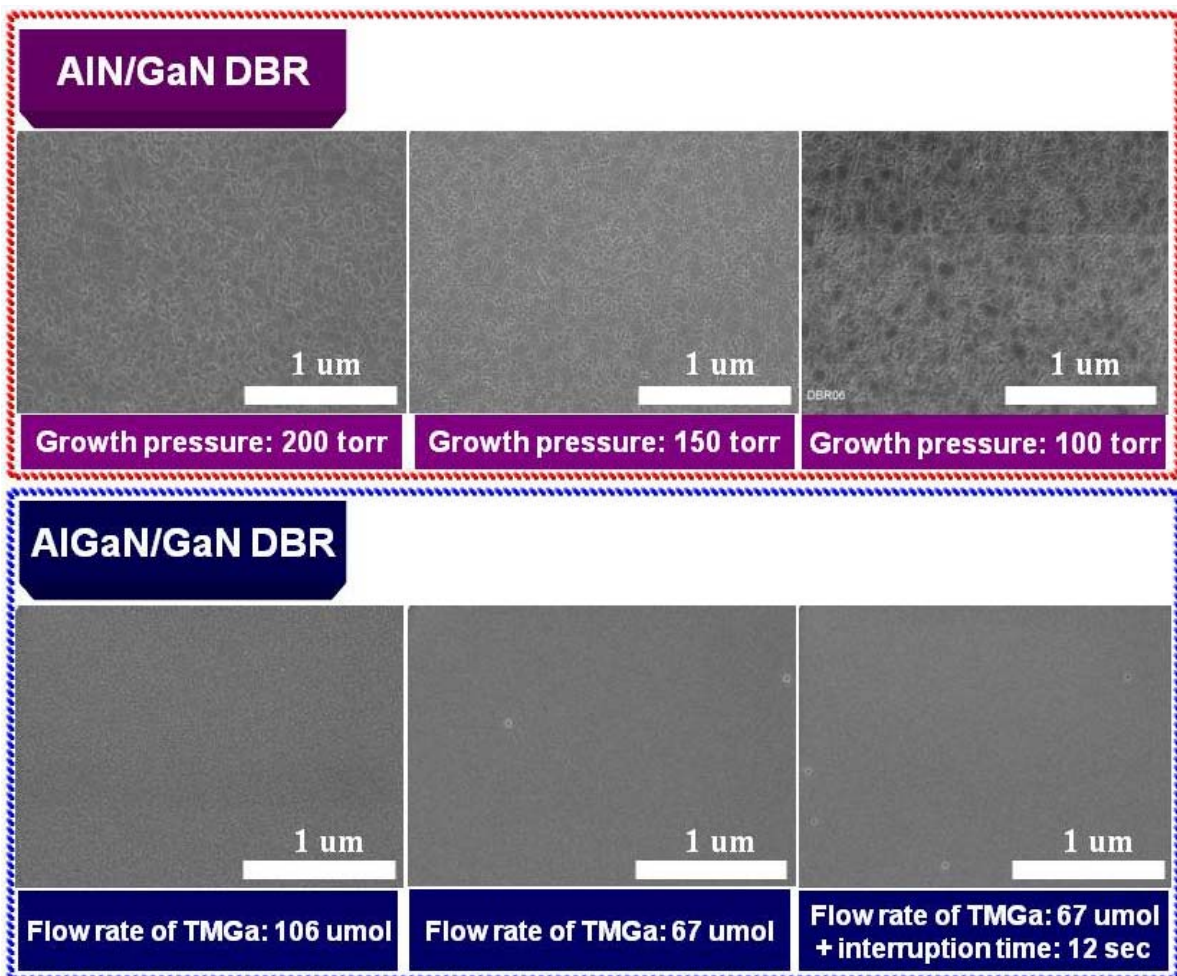


Figure 24. SEM images of 5 pairs of AlN/GaN and AlGaIn/GaN DBRs structures

Figure 25 shows XRD measurements of AlN/GaN and AlGaN/GaN DBRs structures. The thickness of each period (AlGaN/GaN) can be calculated based on the oscillation peak. Additionally, the thickness of one period in $\text{Al}_{0.2}\text{Ga}_{0.8}\text{N}/\text{GaN}$ DBRs should be 81.2 nm for the target wavelength of 400 nm. Therefore, the optimized thickness can be obtained by controlling the growth conditions for 400 nm.

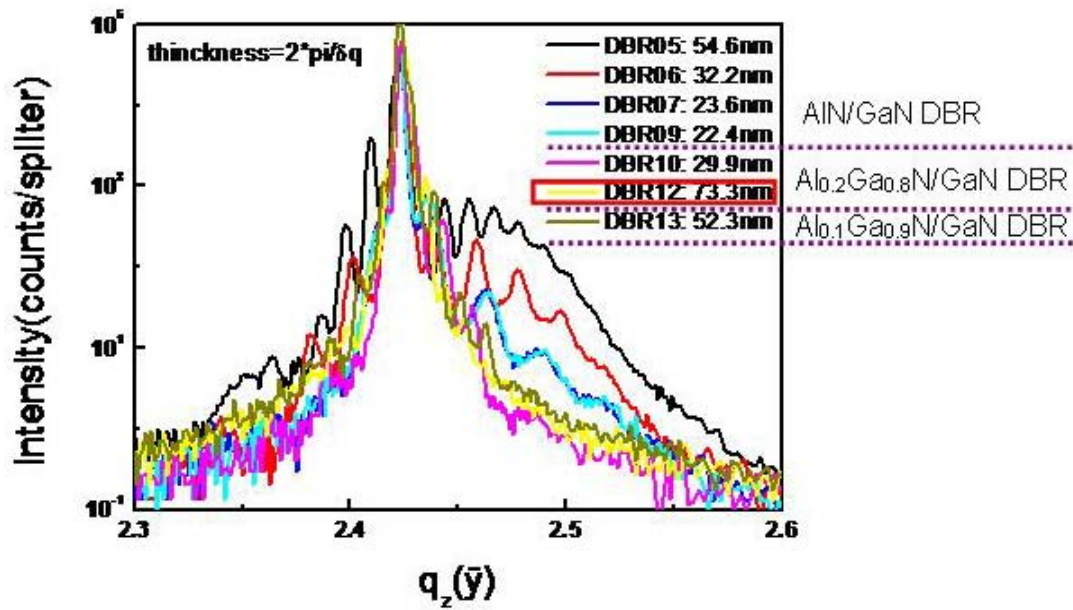


Figure 25. XRD measurements of AlN/GaN and AlGaIn/GaN DBRs structures

The higher reflectivity of DBRs is required to improve the performance of single photon devices. Figure 26 shows the reflectivity of AlGaIn/GaN DBRs with 2 and 5 pairs, respectively.

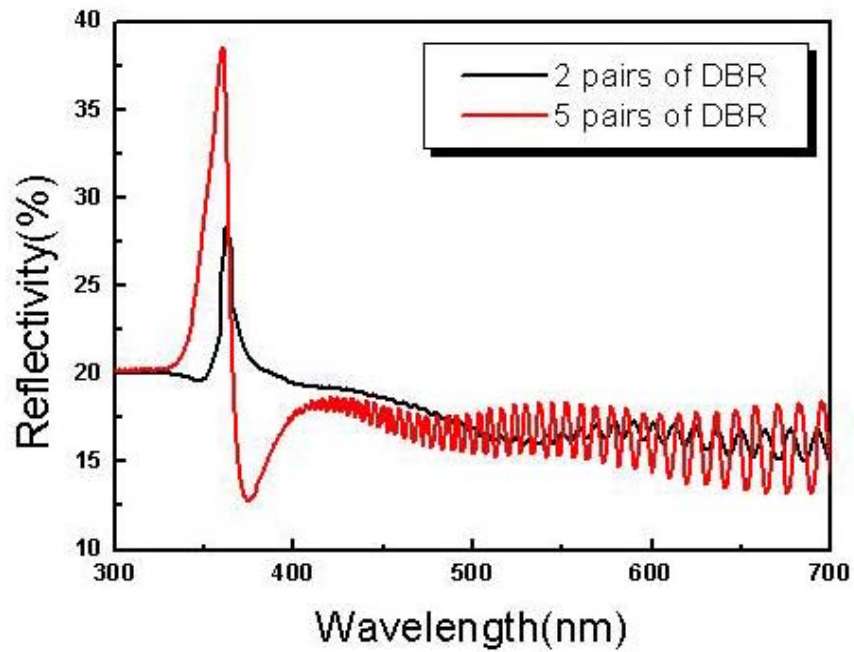


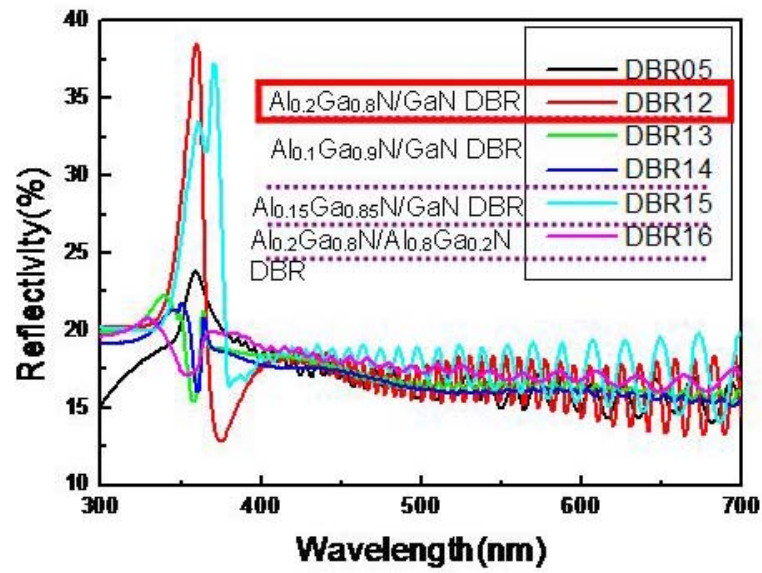
Figure 26. Reflectivity of AlGaIn/GaN DBRs with 2 and 5 pairs

The reflectivity of AlGaN/GaN DBRs with 2 and 5 pairs is 27% and 38%, respectively. The difference in target wavelength is negligibly small in the samples produced by run-to-run process.

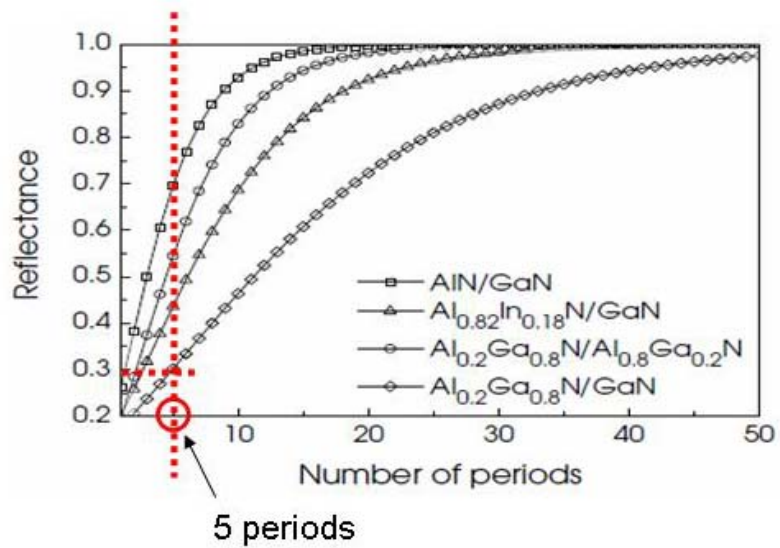
Figures 27 (a) and (b) show the reflectivity of $\text{Al}_x\text{Ga}_{(1-x)}\text{N}/\text{GaN}$ DBRs structures as a function of wavelength and a number of periods, respectively. The reflectivity of $\text{Al}_x\text{Ga}_{(1-x)}\text{N}/\text{GaN}$ DBRs is increased as Al composition is increased. The 5 pairs of $\text{Al}_{0.2}\text{Ga}_{0.8}\text{N}/\text{GaN}$ DBRs instead of 30 pairs show the highest reflectivity of 38% as shown in Fig. 27 (a). This value is higher than the reported reflectance of 5 pairs of $\text{Al}_{0.2}\text{Ga}_{0.8}\text{N}/\text{GaN}$ DBRs structure. The stop band width of $\text{Al}_{0.2}\text{Ga}_{0.8}\text{N}/\text{GaN}$ DBRs structure is 7 nm.

For the high reflectivity of $\text{Al}_x\text{Ga}_{1-x}\text{N}/\text{GaN}$ DBRs, the pairs and Al composition should be increased. However, the increment of Al composition is limited due to the crack problem resulting from a large lattice mismatch. Figure 28 shows SEM images of 30 pairs of $\text{Al}_{0.2}\text{Ga}_{0.8}\text{N}/\text{GaN}$ DBRs structure with a growth interruption time. There are many pits observed on the surface of DBRs without an interruption time. The surface morphology of DBRs is improved as the growth interruption time is increased due to the enhanced surface mobility of Al adatom.

(a)



(b)



Figures 27. Reflectivity of $\text{Al}_x\text{Ga}_{(1-x)}\text{N}/\text{GaN}$ DBRs structures as a function of (a) wavelength and (b) a number of periods (reported)

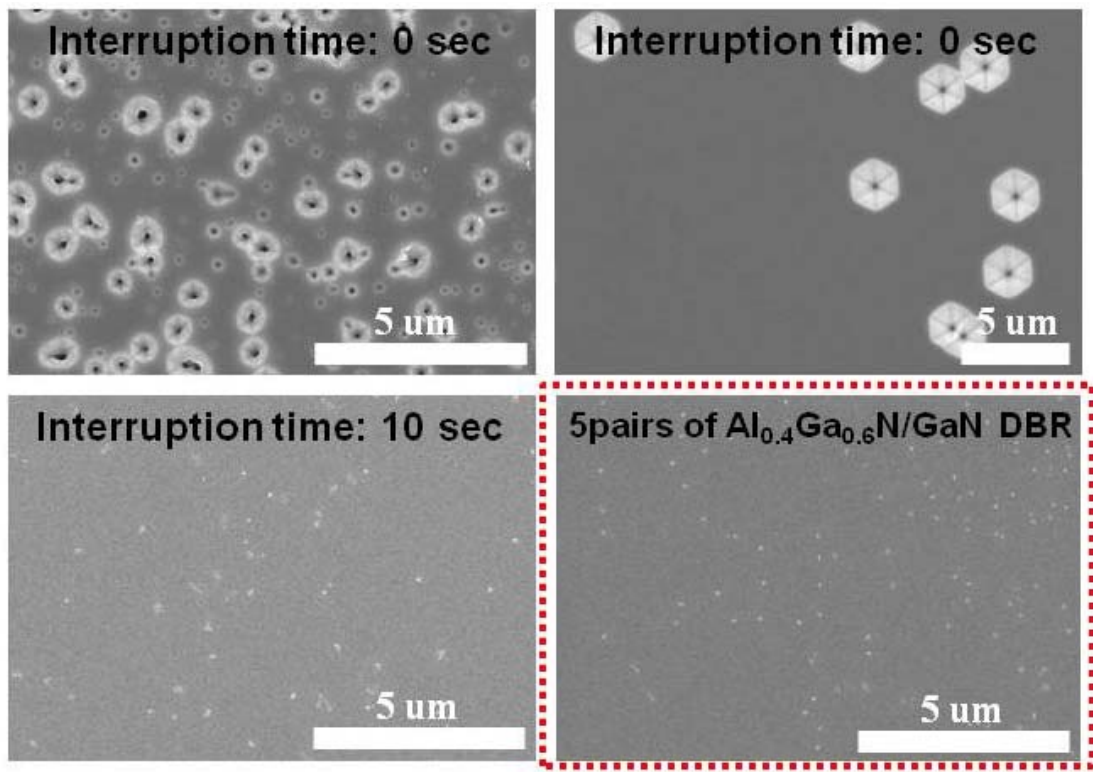
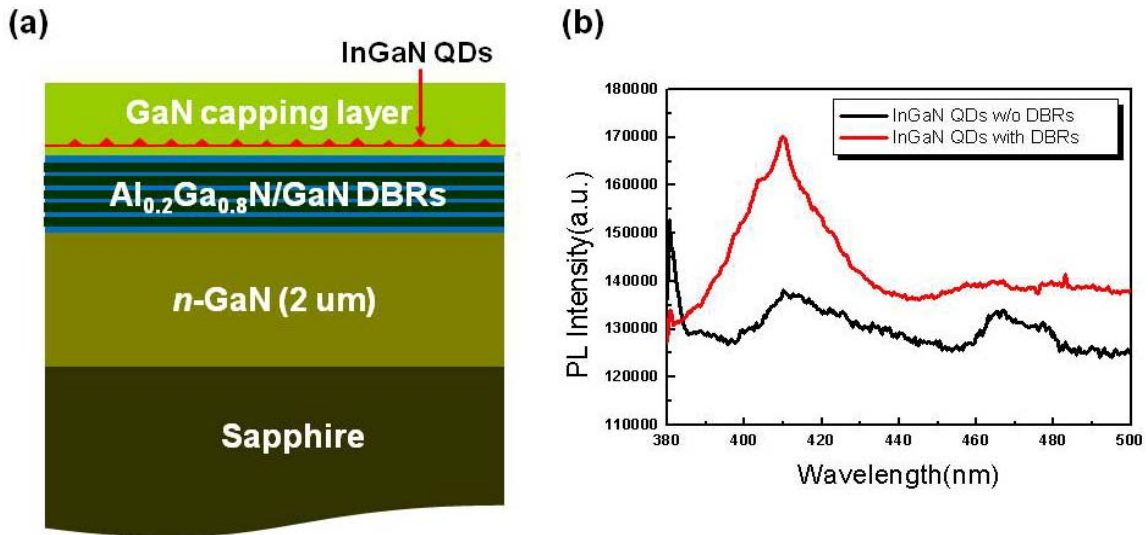


Figure 28. SEM images of 30 pairs of $\text{Al}_{0.2}\text{Ga}_{0.8}\text{N}/\text{GaN}$ DBRs structure with a growth interruption time

Figures 29 (a) and (b) show the schematic diagram of InGaN quantum dots with AlGaN/GaN DBRs structure and PL intensity of InGaN quantum dots without and with AlGaN/GaN DBRs. The growth interruption time is applied to enhance the crystal quality of DBRs and the density of InGaN quantum dots is about $1 \times 10^{10} /\text{cm}^2$. The PL intensity of InGaN quantum dots with DBRs is increased and this is attributed to the reflectivity of AlGaN/GaN DBRs.



Figures 29. (a) Schematic diagram of InGaN quantum dots with AlGa_{0.2}N/GaN DBRs structure and (b) PL intensity of InGaN quantum dots without and with AlGa_{0.2}N/GaN DBRs

4) Summary

The structure is designed for single photon emitting devices by using Rsoft FULLWAVE simulation.

- The reflectivity of 30 pairs of AlGa_{0.2}N/GaN DBRs at 400 nm is 94%.
- The resonant wavelength is obtained at 400 nm in the cavity.

We have optimized the growth conditions of InGaN quantum dots and AlGa_{0.2}N/GaN DBRs.

- The InGaN quantum dots with a small size and low density of $\sim 10^9/\text{cm}^2$ are grown on GaN layer using MOCVD.
- The 5 pairs of Al_{0.2}Ga_{0.8}N/GaN DBRs instead of 30 pairs show the highest reflectivity of 38%.
- The growth interruption time is applied to improve the surface morphology of Al_{0.2}Ga_{0.8}N/GaN DBRs structure.

The emission from InGaN quantum dots with DBRs is characterized using PL measurement.

- The PL intensity of InGaN quantum dots with DBRs is higher than that without DBRs.
- This enhancement shows the possibility for the application to single photon emitting diodes.

10. Software and/or Hardware (if they are specified in the contract as part of final deliverables)

None